

## ESR Spectra of $\text{Cr}^{3+}$ in Axial Symmetry Sites

R. S. DE BIASI, J. A. M. MENDONCA and P. D. PORTELLA

*Instituto Militar de Engenharia, Rio de Janeiro, RJ*

Recebido em 2 de Março de 1980; versão revista recebida em 5 de Novembro de 1980

The resonance fields and peak-to-peak amplitudes of the ESR spectrum of  $\text{Cr}^{3+}$  in axial symmetry have been computed as functions of the zero-field splitting parameter,  $D$ , for three orientations of the magnetic field relative to the symmetry axis:  $0^\circ$ ,  $40^\circ$  and  $90^\circ$ . The results, which are presented in graphical form, may be used for the identification and interpretation of  $\text{Cr}^{3+}$  spectra in single crystals and in polycrystalline materials.

Os campos de ressonância e amplitudes pico-a-pico do espectro de ESR de  $\text{Cr}^{3+}$  em simetria axial foram calculados em função do parâmetro de desdobramento de campo zero,  $D$ , para três diferentes orientações do campo magnético em relação ao eixo de simetria:  $0^\circ$ ,  $40^\circ$  e  $90^\circ$ . Os resultados, que são apresentados em forma de gráficos, podem ser usados para a identificação e interpretação de espectros de  $\text{Cr}^{3+}$  em monocristais e em materiais policristalinos.

### 1. INTRODUCTION

The ESR spectrum of a diamagnetic sample doped with a paramagnetic impurity generally consists of several lines. Some of these lines are due to the dopant, and may correspond to one or more symmetry sites; others are due to unwanted paramagnetic impurities, which are frequently present in significant concentrations. In order to interpret the spectrum, one generally assumes that a particular line or a set of lines is due to a particular ion in a given symmetry site, compatible with the symmetry of the matrix. This initial assumption can then be

checked by predicting the associated spectrum for other orientations and/or for other transitions. There are two characteristic features of a resonance line which are easily measured in a conventional ESR spectrometer with first-derivative presentation: the resonance field,  $H_r$ , and the peak-to-peak amplitude,  $P$ . These can be used together to resolve ambiguities in the spectrum, as it happens when the resonance field is about the same for different ions.

The calculation of resonance fields and peak-to-peak amplitudes for arbitrary angles and symmetries is a cumbersome procedure, which involves the diagonalization of the spin Hamiltonian. A simple method to estimate the line positions and amplitudes given a particular set of spin Hamiltonian parameters or, conversely, to estimate the spin Hamiltonian parameters given a particular spectrum, is clearly desirable. In the present work, such a method is developed for a spin  $S = 3/2$  in axial symmetry. It consists in generating a set of graphs for the resonance fields and relative amplitudes as functions of the zero-fields splitting parameter,  $D$ , for selected angles between the magnetic field and the crystal  $c$ -axis.

The ions likely to have a spin angular momentum of  $3/2$  are  $V^{2+}$ ,  $Cr^{3+}$  and  $Mn^{4+}$ . The principal isotopes of vanadium and manganese have a nonzero nuclear spin and this leads to hyperfine splitting, which is not included in the calculations that follow. The direct application of the present work is therefore restricted to  $Cr^{3+}$ .

## 2. THEORY

### 2.1. Spin Hamiltonian

The energy levels of the ground state of  $Cr^{3+}$  ( $S=3/2$ ) in axial symmetry can be described by the spin Hamiltonian :

$$H = g_{\parallel} \beta H_z S_z + g_{\perp} \beta (H_x S_x + H_y S_y) + D [S_z^2 - S(S+1)/3] \quad (1)$$

where  $H_z$ ,  $H_x$  and  $H_y$  are the components of the applied field,  $\beta$  is the

Bohr magneton,  $g_{\parallel}$ , and  $g_{\perp}$  are the spectroscopic splitting factors,  $D$  is the zero-field splitting parameter and the  $z$  axis is taken along the crystal  $c$ -axis. The difference between  $g_{\parallel}$ , and  $g_{\perp}$  is usually very small<sup>2</sup> and will be neglected in the calculation that follow. In the case of  $\text{Cr}^{3+}$ , the assumption that  $g_{\parallel} = g_{\perp} = g = 1.98$  is a fairly good approximation<sup>2</sup>.

To perform the necessary calculations we have rewritten the Hamiltonian of eq. (1) in a laboratory system of reference axes,  $x'$ ,  $y'$ ,  $z'$ , where the  $z'$  axis is along the applied field  $L$ . The  $y'$  axis is chosen to coincide with the  $y$  axis. If the applied field  $L$  makes an angle  $\theta$  with the  $c$ -axis, the laboratory coordinates  $x'$ ,  $y'$ ,  $z'$  of a point  $x$ ,  $y$ ,  $z$  in the unprimed system are given by

$$\begin{aligned}x' &= x \cos\theta + z \sin\theta \\y' &= y \\z' &= -x \sin\theta + z \cos\theta\end{aligned}\tag{2}$$

The spin operators  $S_x$ ,  $S_y$  and  $S_z$  are transformed to  $S_{x'}$ ,  $S_{y'}$ ,  $S_{z'}$  in the same way as the coordinates. In this coordinate system the spin Hamiltonian becomes

$$\begin{aligned}H &= g\beta HS_{z'} + (1/2)D(3 \cos^2\theta - 1) [S_z^2 - S(S+1)/3] \\&+ D \sin\theta \cos\theta [S_z S_{x'} + S_x S_z] \\&+ (1/2) D \sin^2\theta [S_x^2 - S_y^2]\end{aligned}\tag{3}$$

The parameter  $D$  can be eliminated by writing  $G = g\beta H/D$ , so that, taking  $S = 3/2$ , the Hamiltonian assumes the form

$$\begin{aligned}H &= GS_{z'} + (1/2)(3 \cos^2\theta - 1) (S_z^2 - 15/12) \\&+ \sin\theta \cos\theta [S_z S_{x'} + S_x S_z] \\&+ (1/2) \sin^2\theta [S_x^2 - S_y^2]\end{aligned}\tag{4}$$

## 2.2. Line Amplitudes

The paramagnetic resonance absorption is produced by application of a microwave radiation field  $H_1 \cos \omega t$ , that induces transitions among the energy levels described in the preceding section. In the usual experimental configuration,  $H_1$  is parallel to the  $y^r$  axis. The relative transition probability for a transition between two particular levels,  $i$  and  $j$ , is given by<sup>3</sup>:

$$P_{ij} = g\beta |\langle i | S_y | j \rangle|^2 \frac{\partial H}{\partial h\nu} g_{ij}(H) \quad (5)$$

where  $\nu$  is the microwave frequency and  $g_{ij}(H)$  is the lineshape function.

If the line shape is the same for all transitions, as is frequently the case, the factor  $g_{ij}(H)$  may be dropped from eq. (5). The relative line intensity can thus be written as:

$$I_{ij} = g\beta |\langle i | S_y | j \rangle|^2 \frac{\partial H}{\partial h\nu} \quad (6)$$

If the modulation amplitude is much less than the linewidth, the line intensity  $I_{ij}$  is proportional<sup>4</sup> to the peak-to-peak amplitude of the first-derivative line,  $P_{ij}$ , times the square of the peak-to-peak linewidth,  $\Delta H_{pp}$ :

$$I_{ij} = P_{ij} \frac{\Delta H_{pp}^2}{\nu} \quad (7)$$

In a field swept spectrum, the linewidth is given by<sup>3</sup>:

$$\Delta H_{pp} = \frac{\partial H}{\partial h\nu} \Delta \nu_{pp} \quad (8)$$

where  $\Delta \nu_{pp}$  is the linewidth in a frequency swept spectrum.

According to eqs. (6), (7) and (8), and assuming that  $\Delta \nu_{pp}$  is the same for all transitions, we have:

$$P_{ij} = \frac{g\beta |\langle i | S_y | j \rangle|^2}{\partial H / \partial h\nu} \quad (9)$$

The value of  $\partial H/\partial h\nu$  in eq. (9) is given by<sup>5</sup>:

$$\frac{\partial H}{\partial h\nu} = \frac{1}{g\beta} |\langle i|S_z|j\rangle - \langle j|S_z|i\rangle|^{-1} \quad (10)$$

The relative amplitude may thus be expressed as:

$$P_{i,j} = |\langle i|S_y|j\rangle|^2 |\langle i|S_z|j\rangle - \langle j|S_z|i\rangle| \quad (11)$$

### 3. CALCULATIONS

The matrix derived from the Hamiltonian (4) is given below.

$$H = \begin{array}{l} \langle 3/2| \\ \langle 1/2| \\ \langle -1/2| \\ \langle -3/2| \end{array} \begin{bmatrix} |3/2\rangle & |1/2\rangle & |-1/2\rangle & |-3/2\rangle \\ 1.5G + A & B\sqrt{3} & C\sqrt{3} & 0 \\ B\sqrt{3} & 0.5G - A & 0 & C\sqrt{3} \\ C\sqrt{3} & 0 & -0.5G - A & -B\sqrt{3} \\ 0 & C\sqrt{3} & -B\sqrt{3} & -1.5G + A \end{bmatrix} \quad (12)$$

where

$$\begin{aligned} A &= (3 \cos^2\theta - 1)/2 \\ B &= \sin\theta \cos\theta \\ C &= (\sin^2\theta)/2 \end{aligned} \quad (13)$$

The matrix above was diagonalized with the help of a computer program written in FORTRAN. For a given angle,  $\theta$ , and a given normalized field,  $G$ , the program calculated the parameters  $\bar{W}_{i,j}$ ,  $X_{i,j}$ ,  $P_{i,j}$ , defined as follows.  $\bar{W}_{i,j} = \bar{W}_i - \bar{W}_j$  is the difference in energy between pairs of eigenvalues, expressed in dimensionless units of  $h\nu/D$ .  $X_{i,j} = G/\bar{W}_{i,j} = g\beta H/h\nu$  is the normalized resonance field. It can also be expressed as  $H/H_0$ , where  $H_0 = h\nu/g\beta$  is a convenient parameter.  $P_{i,j}$  is the relative peak-to-peak amplitude, calculated according to eq. (11). By repeating the calculations for several values of  $G$ , it is possible to obtain plots of  $h\nu/D$  vs.  $H/H_0$  and  $P$  vs.  $h\nu/D$  for a given angle  $\theta$ .

Due to practical limitations (at least two plots are needed for each angle) the results are presented for only three angles:  $0^\circ$ ,  $40^\circ$  and  $90^\circ$ . This choice has been made for the following reasons. In the case of single crystals, the sample is generally cut perpendicularly to the  $c$ -axis and the first measurements are taken with the magnetic field parallel and perpendicular to this axis. After the Hamiltonian parameters have been estimated, measurements may be taken at another (arbitrary) angle to check the results. With polycrystals, transitions are usually observed<sup>3</sup> only at the turning points of the Hamiltonian, i.e., at fields where  $\partial H/\partial \theta \sim 0$ . For a spin  $3/2$  in axial symmetry, the turning points occur<sup>5</sup> at  $0^\circ$ ;  $90^\circ$  and an angle between  $35^\circ$  and  $45^\circ$ . The angle of  $40^\circ$  was chosen as a compromise. Graphs for  $\theta=40^\circ$  allow a fairly accurate estimate of the line positions for off-axis transitions in polycrystalline specimens. On the other hand, in the case of polycrystals, the line amplitude depends not only on the single-crystal amplitude at the turning points, but also on the factors  $\sin\theta$  and  $38/30$  (see Reference 3). As a rule, the transitions with turning points at  $\theta=90^\circ$  and  $0 \sim 40^\circ$  are more intense and the transitions with turning points  $\theta=0^\circ$  are weaker (actually, the only transitions that may have turning points at  $0 \sim 40^\circ$  are 2-3 and 1.4).

#### 4. RESULTS

The results of the computations described in the preceding section are shown in Figs. 1-6. The plots of  $WD$  ( $= \hbar\nu/D$ ) as a function of  $H/H_0$  for  $\theta = 0^\circ$ ,  $40^\circ$  and  $90^\circ$  are shown in Figs. 1-3. The plots of  $P$  as a function of  $WD$  for  $\theta = 0^\circ$ ,  $90^\circ$  appear in the same graph, Fig. 4. Figs. 5 and 6 show the relative intensity for  $\theta = 40^\circ$ . The transitions are labeled in terms of the energy levels involved. The energy levels are numbered in order of decreasing energy.

The use of the graphs is illustrated in the examples that follow.

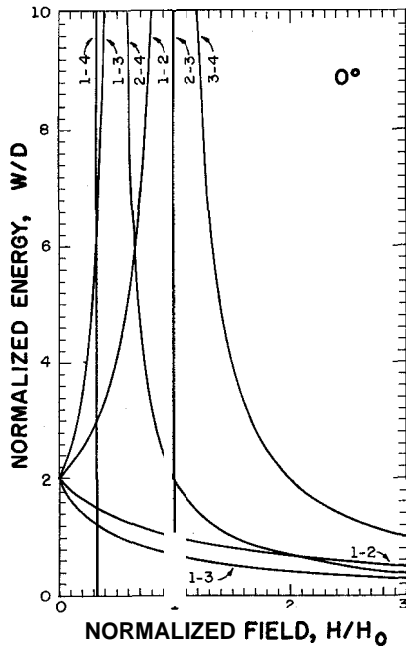


Fig.1 -  $W/D$  as a function of  $H/H_0$  for  $\theta = 0^\circ$

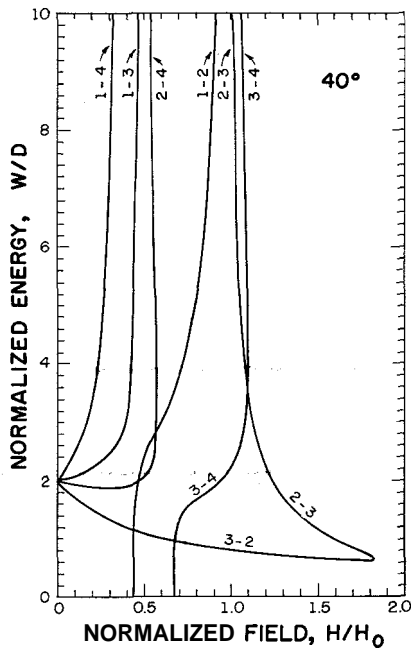


Fig.2 -  $W/D$  as a function of  $H/H_0$  for  $\theta = 40^\circ$ .

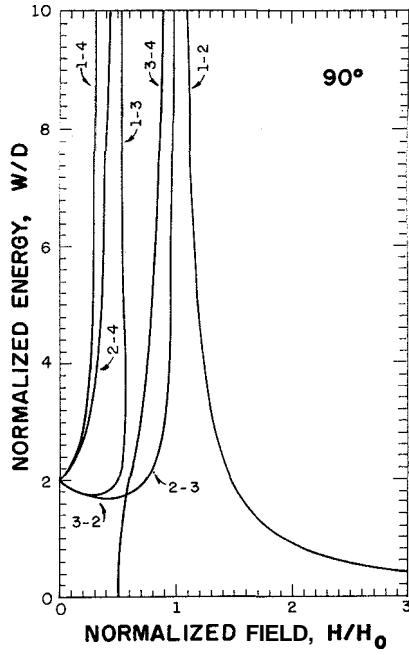


Fig.3 -  $W/D$  as a function of  $H/H_0$  for  $\theta = 90^\circ$ .

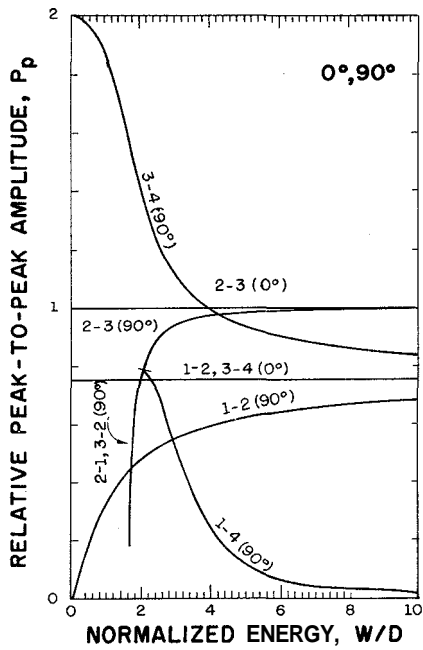


Fig.4 -  $P$  as a function of  $W/D$  for  $\theta = 0^\circ$  and  $\theta = 90^\circ$ .



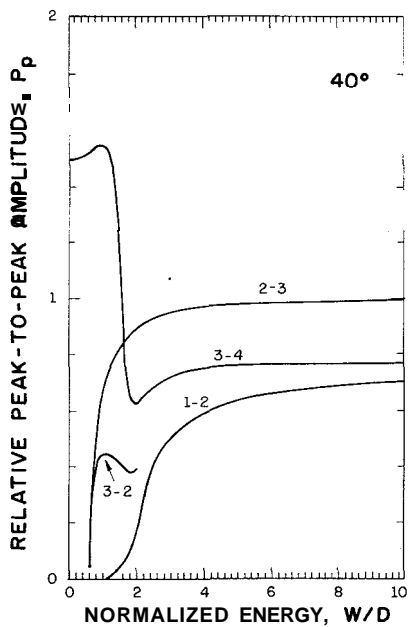


Fig.5 -  $P$  as a function of  $W/D$  for  $\theta = 40^\circ$ ; transitions 1-2, 2-3, 3-2 and 3-4.

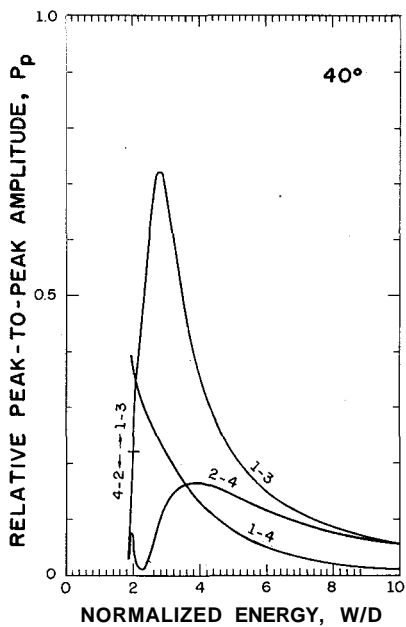


Fig.6 -  $P$  as a function of  $W/D$  for  $\theta = 40^\circ$ ; transitions 1-3, 1-4, 2-4 and 4-2.

## 5. EXAMPLES

### 5.1. ESR of $\text{Cr}^{3+}$ in Single-Crystal $\text{Al}_2\text{O}_3$

#### 5.1.1. Sample Preparation

The  $\text{Al}_2\text{O}_3$  single crystal used in this work was cut from an ingot kindly provided by Prof. Zoraide Arguello of UNICAMP. The ingot was oriented by x-ray diffraction, using Laue's back scattering technique, and sliced with a diamond saw.

#### 5.1.2. Experimental Results and Discussion

The spectrum of a sample of single-crystal  $\text{Al}_2\text{O}_3$  shows several lines, which are attributed to impurities. Chemical analysis shows that the main paramagnetic impurities are  $\text{Cr}^{3+}$  and  $\text{Fe}^{3+}$ . It is not possible to measure the line positions with good accuracy at  $\theta=0^\circ$ , because some lines are partially superposed. At  $\theta = 90^\circ$ , the spectrum is much simpler (Fig.7a): it consists of four well-separated lines, that for a microwave frequency of 9.25 GHz appear at fields of 1325, 1954, 3369 and 5387 gauss.

We begin by assuming that  $g = 1,98$ , so that, with  $\nu = 9,25$  GHz, we get  $H_0 = h\nu/g\beta = 3428$  gauss. The normalized fields for the four lines are thus  $H/H_0 = 0.39, 0.57, 0.98$  and  $1.57$ . If the line with  $H/H_0 = 1.57$  (line D) is attributed to the  $\text{Cr}^{3+}$  ion in axial symmetry, it can be due only to the 1-2 transition (see Fig.3). If this is the case,  $W/D \sim 1.60$  and a second line (transition 3-4) is predicted at  $H/H_0 \sim 0.55$ , i.e., at  $H \sim 1900$  gauss. Since a line is found near the predicted position (line B), this hypothesis seems to be correct. Moreover, no other transitions should be observed, and therefore the lines at  $H/H_0 = 0.39$  and  $0.98$  (lines A and C) are attributed to the  $\text{Fe}^{3+}$  ion.

As a check, one may compare the predicted line positions at  $\theta = 40^\circ$  with the experimental results. This spectrum is shown in Fig. 7b. According to Figs. 2,5 and 6, three lines should be observed, corresponding to transitions 3-2, 3-4 and 2-3, at fields of 390, 2690

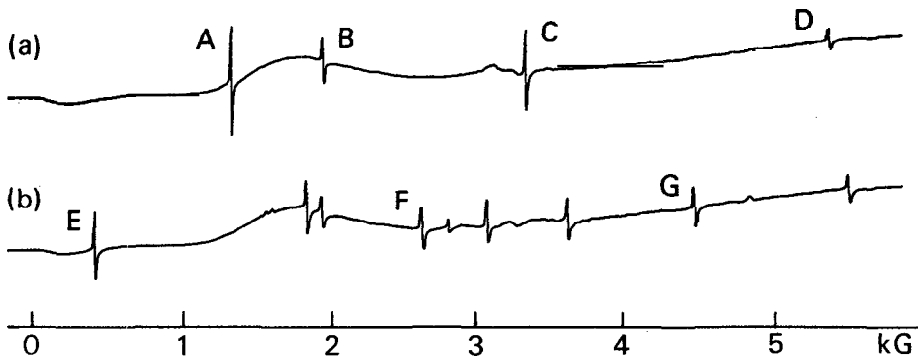


Fig.7 - ESR spectra of a sample of single-crystal  $\text{Al}_2\text{O}_3$  containing Cr and Fe as impurities (room temperature,  $\nu = 9.25$  GHz). (a)  $\theta = 90^\circ$ ; (b)  $\theta = 40^\circ$ . Field values for the  $\text{Cr}^{3+}$  lines, in gauss: A, 1325; B, 1954; C, 3369; D, 5387; E, 395; F, 2670; G, 4510.

and 4520 gauss. Three lines are indeed found near these positions (lines  $E, F, G$ ). The line corresponding to the 1-2 transition is not seen due to its low amplitude (see Fig. 5). All other lines in Fig. 7b are due to  $\text{Fe}^{3+}$  ions.

The best estimates from this analysis are therefore:

$$g = 1.98$$

$$|D|/\hbar = \nu/1.60 = 5.78 \text{ GHz}$$

where D is expressed in frequency units.

The best experimental values for the Hamiltonian parameters of  $\text{Cr}^{3+}$  in  $\text{Al}_2\text{O}_3$ , obtained by fitting the experimental results for several angles in high-purity crystals, are<sup>5</sup>:

$$g_{\parallel} = 1.9817$$

$$g_{\perp} = 1.9819$$

$$|D|/\hbar = 5.747 \text{ GHz}$$

## 5.2. ESR of $\text{Cr}^{3+}$ in Polycrystalline $\text{MgO}$

### 5.2.1. Sample Preparation

The chromium-doped  $\text{MgO}$  sample used in this work was prepared from pure oxides carefully grinding them together and then firing the mixture for 96 hours at  $1350^{\circ}\text{C}$ . Actual chromium concentration was determined by x-ray fluorescence spectrometry to be 0.8 cation%  $\text{Cr}$ .

### 5.2.2. Experimental Results and Discussion

The spectrum of a chromium-doped sample of  $\text{MgO}$  powder (Fig. 8) shows, beside a strong line at 3338 gauss, due to the  $\text{Cr}^{3+}$  ion in cubic symmetry<sup>6</sup>, weaker lines at 712, 2560, 3233, 3712 and 4317 gauss, which are attributed to the  $\text{Cr}^{3+}$  ion in lower symmetry sites.

In order to find out whether some or all of these lines are due to  $\text{Cr}^{3+}$  in axial symmetry, we begin by assuming that the strongest

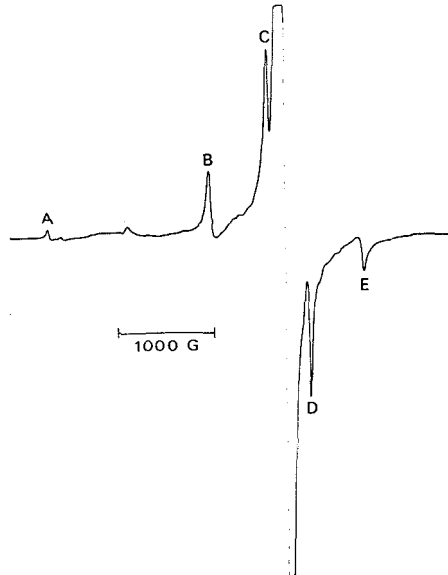


Fig.8 - ESR spectrum of a sample of  $\text{MgO}$  powder containing 0.8 cation%  $\text{Cr}^{3+}$  (room temperature,  $\nu = 9.25$  GHz). Field values for the axial spectrum, in gauss: A, 712; B, 2560; C, 3233; D, 3712; E, 4317. The central, high-amplitude line is due to  $\text{Cr}^{3+}$  ions in cubic symmetry sites.

line, at 3712 gauss, is due to a  $\theta = 90^\circ$  turning point. The normalized field for this line, using the same value for  $H$ , as in the preceding example, is  $H/H_0 = 1.08$ . According to Fig. 3, a line with  $H/H_0 \sim 1.0$  could be attributed to transition 2-3 with a low value of  $D$ , of the order of 0.1 W. In that case, however, Figs. 3 and 4 show that another high-amplitude transition, transition 3-4, should be observed in the neighborhood of  $H/H_0 = 0.9$ , i.e.,  $H = 3085$ . Since this line is not seen, our initial assumption is clearly wrong.

In the next try, we assign the second most intense line, the one at 3233 gauss, to a  $\theta = 90^\circ$  turning point. The normalized field is  $H/H_0 = 0.94$ . According to Fig. 3, a line with  $H/H_0 \sim 0.95$  could be attributed to transition 2-3 with  $W/D \sim 4$ . Figures 3 and 4 show that if this assignment is correct, other strong lines should be observed at  $H/H_0 = 0.75$  (transition 3-4) and  $H/H_0 = 1.25$  (transition 1-2). The corresponding fields are 2571 and 4285 gauss. Since two lines are found near the predicted positions, our assumption is probably correct.

As a check, we use Figs. 2 and 5 to predict the positions of other high-amplitude lines in the spectrum. Since we know<sup>5</sup> that the only transitions that may have turning points at  $\theta \sim 40^\circ$  are 2-3 and 1-4, the off-axis transitions are predicted to occur at  $H/H_0 = 0.2$  (transition 1-4) and  $H/H_0 = 1.1$  (transition 2-3). The corresponding fields are 686 and 3771 gauss. Two lines are indeed found near the predicted positions (lines A and D in Fig. 8).

The lines corresponding to the turning points at  $\theta = 0^\circ$  are too weak to be observed in the scale of Fig. 8. If the gain of the instrument is increased, however, additional lines are seen near the positions predicted with the help of Figs. 1 and 4.

All lines in the spectrum of Fig. 8, except the central strong line, can thus be attributed to the  $\text{Cr}^{3+}$  ion in axial symmetry. The Hamiltonian parameters are estimated to be:

$$g = 1.98$$

$$|D|/h = \nu/4.00 = 2.31 \text{ GHz}$$

The experimental values for the Hamiltonian parameters of  $\text{Cr}^{3+}$  in axial symmetry sites in  $\text{MgO}$ , obtained from single-crystal work, are<sup>7</sup>:

$$g_{\parallel} = g_{\perp} = 1.9782$$

$$|D|/h = 2.45 \text{ GHz}$$

## 6. CONCLUSIONS

The examples of the preceding section show that with the help of the graphs presented in this work it is possible to identify the lines due to the  $\text{Cr}^{3+}$  ion in axial symmetry sites, both in single crystals and in polycrystalline materials. It is also possible to estimate the value of the zero-field splitting parameter,  $D$ , with fairly good accuracy.

## REFERENCES

1. B. Bleaney and K.W.H. Stevens, *Rep. Progr. Phys.* 16, 108 (1953).
2. J. E. Wertz and J. R. Bolton, *Electron Spin Resonance* (McGraw-Hill, New York, 1972), Chapter 11.
3. G. van Veen, *J. Magn. Resonance* 30, 91 (1978).
4. J. S. Hyde, *Experimental Techniques in EPR* (Varian, Palo Alto, 1963), p. 10.
5. T. T. Chang, D. Foster, and A. H. Kahn, *NBS J. of Research* 83, 133 (1978).
6. W. Low, *Phys. Rev.* 105, 801 (1957).
7. J. E. Wertz and P. Auzins, *J. Phys. Chem. Solids* 28, 1557 (1967).